Tree Physiology 00, 1–15
doi:10.1093/treephys/tpz016

Research paper

Drought response strategies and hydraulic traits contribute to mechanistic understanding of plant dry-down to hydraulic failure

Chris J. Blackman[1,7], Danielle Creek[1], Chelsea Maier[1], Michael J. Aspinwall[1,2], John E. Drake[1,3], Sebastian Pfautsch[1,4], Anthony O'Grady[5], Sylvain Delzon[6], Belinda E. Medlyn[1], David T. Tissue[1] and Brendan Choat[1]

[1]Hawkesbury Institute for the Environment, Western Sydney University, Locked Bag 1797, Penrith NSW 2751, Australia; [2]Department of Biology, University of North Florida, 1 UNF Drive, Jacksonville, FL 32224, USA; [3]Forest and Natural Resources Management, SUNY-ESF, 1 Forestry Drive, Syracuse, NY 13210, USA; [4]School of Social Science and Psychology (Urban Studies), Western Sydney University, Locked Bag 1797, Penrith, NSW 2751, Australia; [5]CSIRO Land and Water, Hobart TAS 7001, Australia; [6]BIOGECO, INRA, Univ. Bordeaux, 33615 Pessac, France; [7]Corresponding author (c.blackman@westernsydney.edu.au)

Received October 10, 2018; accepted 0, 0; handling Editor Frederick Meinzer

Drought-induced tree mortality alters forest structure and function, yet our ability to predict when and how different species die during drought remains limited. Here, we explore how stomatal control and drought tolerance traits influence the duration of drought stress leading to critical levels of hydraulic failure. We examined the growth and physiological responses of four woody plant species (three angiosperms and one conifer) representing a range of water-use and drought tolerance traits over the course of two controlled drought–recovery cycles followed by an extended dry-down. At the end of the final dry-down phase, we measured changes in biomass ratios and leaf carbohydrates. During the first and second drought phases, plants of all species closed their stomata in response to decreasing water potential, but only the conifer species avoided water potentials associated with xylem embolism as a result of early stomatal closure relative to thresholds of hydraulic dysfunction. The time it took plants to reach critical levels of water stress during the final dry-down was similar among the angiosperms (ranging from 39 to 57 days to stemP_{88}) and longer in the conifer (156 days to stemP_{50}). Plant dry-down time was influenced by a number of factors including species stomatal-hydraulic safety margin (g_sP_{90} – stemP_{50}), as well as leaf succulence and minimum stomatal conductance. Leaf carbohydrate reserves (starch) were not depleted at the end of the final dry-down in any species, irrespective of the duration of drought. These findings highlight the need to consider multiple structural and functional traits when predicting the timing of hydraulic failure in plants.

Keywords: drought, *eucalyptus*, hydraulics, mortality, NSCs, *Pinus*, rainfall exclusion, rainout shelter, recovery.

Introduction

Regional-scale forest dieback resulting from severe and prolonged drought has profound effects on community composition and species interactions, with feedbacks to surface hydrology and ecosystem carbon balance (Breda et al. 2006, Reichstein et al. 2013, Clark et al. 2016). Drought-induced tree mortality events at local and/or large scales are now well documented in nearly all forested biomes across the globe (Fensham and Holman 1999, Breda et al. 2006, Allen et al. 2010, Phillips et al. 2010, Duke et al. 2017). However, in many instances, the rate and/or extent of mortality varies, even among co-occurring species, suggesting species vary strongly in traits that define different drought response strategies and that influence drought survivorship thresholds (Breshears et al. 2005, Engelbrecht et al. 2007, Fensham and Fairfax 2007, Poot and Veneklaas 2013, Johnson et al. 2018). Given that the frequency and intensity of drought are projected to increase with rising temperature under climate change (Engelbrecht 2012, Allen et al. 2015),

there is an urgent need to better understand how contrasting drought response strategies and different plant traits influence the timing and mechanisms of drought mortality (Choat et al. 2018).

The risk of death during drought is broadly determined by the capacity of plants to minimize their exposure to lethal thresholds of carbon depletion and/or hydraulic failure due to drought-induced cavitation (McDowell et al. 2008, Sala et al. 2012, Choat 2013). Species that maintain plant water status at relatively safe levels via stringent stomatal control may be vulnerable to carbon depletion, especially under chronic drought conditions, while species that maintain open stomata and allow water potentials to drop close to critical thresholds of xylem cavitation may be more vulnerable to desiccation and catastrophic hydraulic failure. While this relatively simple conceptual framework has been useful in generating hypotheses about mechanisms of drought mortality, recent empirical work predominantly links mortality to hydraulic failure and is so far ambiguous regarding carbon starvation (Anderegg et al. 2012, Mitchell et al. 2013, Duan et al. 2014, 2015, Adams et al. 2017, Choat et al. 2018). Nevertheless, the dynamics of water loss and carbon depletion leading to mortality during drought are complex, with the relative influence of carbon and hydraulic mechanisms of mortality being dependent on a range of plant traits and environmental conditions (Nardini et al. 2016, Adams et al. 2013, 2017, Duan et al. 2018).

Trade-offs between carbon and hydraulic traits that influence water-use, growth and drought response strategies are also likely to influence the duration of drought stress and thus the possible mechanism of mortality (Martinez-Vilalta and Garcia-Forner 2017, Martin-StPaul et al. 2017). For example, fast-growing tree species with high rates of photosynthesis and high rates of hydraulic conductance (see Markesteijn et al. 2011, Reich 2014, Bourne et al. 2017) tend to be susceptible to drought-induced hydraulic failure in accordance with the widely reported trade-off between high levels of hydraulic efficiency and high levels of cavitation resistance (Gleason et al. 2016). However, species with low drought tolerance also tend to exhibit stringent stomatal control (Bartlett et al. 2016, Fu and Meinzer 2018) and thus are not necessarily more at risk of rapid dehydration during drought. In contrast, cavitation-resistant species tend to be slow growing, with xylem anatomical traits such as high xylem cell-wall reinforcement (Hacke et al. 2001) and high fibre-wall area (Jacobsen et al. 2005) that also contribute to high wood density. Consequently, they also tend to show low levels of hydraulic capacitance (Scholz et al. 2011), which is regarded as a drought avoidance trait (Barnard et al. 2011), and thus may have a limited capacity to buffer decreases in water potential during drought. While many of these traits have been incorporated into hydraulic models of the time it takes plants to reach critical levels of drought stress (Ψ_{crit}) (Gleason et al. 2014, Blackman et al. 2016, Martin-StPaul et al. 2017), very few studies have examined multiple traits that contribute to determining plant dry-down times to Ψ_{crit} and tested whether the duration of drought stress influences levels of carbohydrate depletion.

In this study, we examined growth and physiological responses of saplings of four tree species to a series of drought and recovery cycles, followed by an extended period of soil drying to complete canopy browning. The four species included three angiosperms with different eco-hydrological niches and one conifer. The species were chosen to represent a range of growth, water-use and drought tolerance traits, and thus were expected to exhibit different growth and drought response strategies that would influence the timing and mechanism of mortality during extended drought. For each species, we characterized a range of traits linked to drought tolerance, including stem hydraulic vulnerability, stomatal regulation and leaf pressure–volume dynamics. At the end of the final dry-down period, we tested for changes in whole-plant biomass ratios and leaf non-structural carbohydrates (NSCs). We anticipated that longer dry-down times to critical levels of drought stress (Ψ_{crit}) would be linked to traits associated with high drought tolerance either via drought avoidance (e.g., early stomatal closure or high hydraulic capacitance) or drought resistance (e.g., low hydraulic vulnerability to embolism). In either case, we hypothesized that in delaying the onset of Ψ_{crit}, species with longer dry-down times would show higher levels of depletion of carbohydrate reserves.

Materials and methods

Study site

The study took place at the rainout shelters at the Hawkesbury Institute for the Environment in Western Sydney (Australia) (33.61° S, 150.74° E) at elevation 25 m above sea level. The local climate is warm-temperate, with a mean annual temperature of 17 °C and a mean annual rainfall of 730 mm (Bureau of Meteorology, station 067105, 5 km away). The experimental set up included six rainout shelters designed to contain plants up to 6 m tall. The shelter was constructed of steel/metal frame (12 m long × 8 m wide × 6 m height) with a roof pitch of 30°. The roof curtains of the shelters are made of Svennson LS solar-woven ultra™ on a roll-up system and the side curtains are made of Svennson QLS ABRI™ on a concertina system. Sides remain open when there is no rain to allow the continuous flow of air and minimize variation from ambient outside temperature and humidity. The roof and side curtains deploy when rain is detected by a rain sensor measuring the resistance between two electrodes. Natural rain is collected in 50,000 l tanks that retain the chemical properties of precipitation, which was supplementally re-applied to the pots when required.

Species

Three angiosperms (*Casuarina cunninghamiana* Miq., *Eucalyptus sideroxylon* A.cunn. ex Woolls and *Eucalyptus teriticornis* Sm.,

hereafter referred to as Cacu, Eusi and Eute, respectively) and one gymnosperm (*Pinus radiata* D.Don, hereafter referred to as Pira) were chosen for this experiment. Given its occurrence in riparian habitats, we anticipated Cacu would exhibit traits associated with high rates of water-use and low drought tolerance. Eute is widespread along coastal eastern Australia with populations that extend inland and are more exposed to drought. Eusi is a component of dry sclerophyll forest occurring further inland in south-eastern Australia, extending into sites that receive <400 mm of rain annually and was expected to show strong drought tolerance. Pira is native to coastal California, and is an important plantation species in south-eastern Australia. It was chosen to provide a contrast to the three Australian natives on the basis that the species is known to show strong stomatal regulation during drought (Brodribb and McAdam 2013, Mitchell et al. 2013, Duan et al. 2015). Seedlings were purchased from local nurseries and transplanted into 75 l pots and placed within the shelters. The pots contained moderately fertile sandy loam top soil, local to dry sclerophyll forest in Menangle, NSW, Australia (for further details on soil characteristics see Drake et al. 2015, 2017, Dijkstra et al. 2016). All plants were hand-watered to keep soil water content 'well-watered' (i.e., above 14% soil water content) for the first 11 months, while the plants grew to sufficient size.

Experimental design

A total of 16 potted saplings of each species were placed within each of the six rainout shelters. Within each shelter, an equal number of plants of each species were randomly assigned to either a well-watered or drought treatment. Throughout the experiment, well-watered plants were maintained at field capacity via a combination of drip irrigation and manual watering. During the controlled drought treatment phases (see below), soil volumetric water content was measured every other day using a handheld Hydrosense probe (Campbell Scientific, Townsville, QLD, Australia) and water was manually added back to reach the desired level of water deficit.

In this study, we implemented a series of drought and recovery cycles followed by an extended and extreme soil drying event, as previously described by Drake et al. (2017). In brief, the study progressed in four phases. (i) Establishment phase: seedlings were grown in well-watered conditions for close to 1 year, from 10 November 2011 to 18 October 2012. At the end of this phase, the mean plant height was 113, 98, 77 and 63 cm for Cacu, Eute, Eusi and Pira, respectively. (ii) First drought–recovery cycle: for plants assigned to the drought treatment, a controlled dry-down was implemented over 4 weeks, from 18 October to 15 November 2012, such that each pot was dried-down at the same rate to a target soil volumetric water content (VWC) of 0.06 $m^3\ m^{-3}$, which was sufficiently low to elicit a strong physiological response relative to control plants (e.g., a reduction in stomatal conductance (g_s), see Drake et al. 2017), followed by a 10 day recovery phase during which time plants were well-watered. (iii) Second drought–recovery cycle: from 25 November 2012 a second 4-week long dry-down was imposed, with the same specifications as the first, followed by a 4-week well-watered recovery period. (iv) Final dry-down: an extended and extreme drought was initiated on 26 January 2013 and progressed with an initial controlled step-down drought over 6 weeks to a target VWC of 0.06 $m^3\ m^{-3}$, after which water was completely withheld. At the start of this final dry-down phase, the mean plant height was 163, 105, 139 and 101 cm for Cacu, Eute, Eusi and Pira, respectively.

Leaf water potential and canopy leaf death

Leaf water potential was measured at pre-dawn (ψ_{pd}) and mid-day (ψ_{md}) in a sub-sample of one target representative individual chosen of each species per treatment per shelter (48 plants in total). Repeated measurements on the same target individuals were taken immediately prior to and at the peak of each of the drought–recovery cycles, as well as at multiple time points (5 for the three angiosperms and 10 for Pira) during the final dry-down to mortality targeting the same individual on each occasion. For each measurement, one leaf (or cladode in the case of Cacu, and fascicle in the case of Pira) per target individual was taken to limit excessive leaf removal. For plants of Eute, which of the four species had the largest leaves, <10% of total leaf area was removed for leaf water potential measurements over the course of the experiment. Leaves were immediately sealed in a zip-lock bag containing a piece of dampened paper towel and placed in a chiller box and transported to a Scholander-type pressure chamber (Model 600; PMS Instrument Company, Corvallis, OR, USA) for water potential determination.

We also monitored canopy leaf death during the final dry-down phase in the same sub-sample of saplings of each species used to monitor leaf water potential. On each date, we gave each plant a score of between 0 (no browning) and 4 (completely brown) that corresponded to the proportion of canopy leaves that were deemed to be dead (based on their level of leaf brownness); 0 = 0%, 1 = 25%, 2 = 50%, 3 = 75% and 4 = 100%.

Leaf gas exchange

We measured leaf gas exchange at multiple time points during all phases of the experiment, on the same individuals targeted for water potential. On each occasion, leaf-level photosynthesis (A_{sat}) and stomatal conductance (g_s) was measured between 10 am and 2 pm with six identical gas exchange systems (Li-6400, Li-Cor Inc., Lincoln, NE, USA). All photosynthetic parameters were expressed on a projected leaf area basis. Reference CO_2 was set at 400 μmol mol^{-1}, block temperature was set at 25 °C, desiccant dial was turned to full bypass and the light intensity within the 2 × 3 cm cuvette was set at 1800 μmol $m^{-2}\ s^{-1}$. These measurements were previously reported by Drake et al. (2017). The average minimum rate of g_s was determined for each species from gas exchange measurements

taken on the penultimate measurement date of each species respective final dry-down.

Hydraulic vulnerability

Stem hydraulic vulnerability curves were generated for each of the three angiosperm species using bench dehydration (Sperry et al. 1988), and for the conifer Pira using a cavitron (Cochard et al. 2005). The cavitron was not suitable to measure hydraulic vulnerability in the three angiosperm species because of their long vessel length (Choat et al. 2010, Torres-Ruiz et al. 2014). However, numerous studies have demonstrated that the cavitron technique provides accurate estimates of hydraulic vulnerability for conifer species (Cochard et al. 2005, 2010, Choat et al. 2016). Thus, estimates of vulnerability derived from the two measurement techniques are valid for the species to which they were applied and are directly comparable (Cochard et al. 2013). For all species, the entire above-ground component of four to six well-watered plants, each from a different shelter, was excised during early morning in February 2013. For the three angiosperms, main stems (>1 m) were sufficiently long to avoid open vessels in the upper canopy where smaller diameter stem segments were sampled for hydraulics measurements. Following excision, whole branches were transported to the lab in humidified plastic bags and their bases immediately re-cut under water. The cut end of each branch was kept submerged for a minimum of 2 h to ensure water potentials were relaxed within the stem and avoid possible excision artefacts (Wheeler et al. 2013, Torres-Ruiz et al. 2015). After stem xylem tension was determined to be close to zero, by measuring water potentials in two leaves that had been covered in aluminium foil, each branch was placed on the bench and a small diameter stem, approximately 10 cm in length, was sampled by cutting back from the distal end of the branch while submerged under water. The stem sample was shaved at both ends with a fresh razor before being connected to the hydraulics apparatus. Stem hydraulic conductivity measurements were made before and after removal of embolism using a filtered (0.22 μm) solution of distilled water with 2 mmol KCl. Flow rates were logged with a digital liquid flow metre (LiquiFlow L10, Bronkhorst High-Tech BV, Ruurlo, Gelderland, The Netherlands) in conjunction with flow analysis programs FlowDDE (v. 4.69) and FlowPlot (v. 3.34). Any embolisms were removed by flushing the stem for a minimum of 30 min at constant pressure (150 KPa). The relative difference in flow (PLC, percent loss of conductivity) before and after flushing was plotted against stem Ψ. A total of four to six stem segments were sampled from each branch across a range of water potentials, from near zero to those associated with 100% PLC as branches slowly dehydrated over 3–4 days in the lab.

Stem hydraulic vulnerability curves for Pira were generated at the Caviplace platform of the University of Bordeaux using the cavitron technique (Cochard et al. 2005). The main axis of each individual was harvested 50 mm above the soil early in the morning and trimmed to 400 mm in length. Stems were wrapped in moist paper towel and plastic and immediately shipped to France. Samples arrived 2 days after shipping and were immediately refrigerated at 5 °C. Within 2 weeks after receipt of the samples, vulnerability curves were assessed with the cavitron. Before measurement, all branches were cut under water to a standard length of 270 mm. Centrifugal force was used to generate negative pressure in the xylem and to provoke water stress-induced cavitation using a custom rotor mounted on a 'late' centrifuge (HS18; MSE Scientific, London, UK). Xylem conductance was measured under negative pressure using a reference ionic solution of 10 mmol l^{-1} KCl and 1 mmol l^{-1} $CaCl_2$ in deionized water. Xylem pressure (P in MPa) was first set to a reference pressure (−1 MPa) and the maximal hydraulic conductivity (K_{max} in m^2 MPa^{-1} s^{-1}) was determined. The xylem pressure was then set to a more negative pressure by steps of 1 MPa and the hydraulic conductivity K was determined. Data acquisition and processing were performed using the Cavisoft software (Cavisoft v1.5, University of Bordeaux, Bordeaux, France).

Pressure–volume analyses

A terminal branch (from the upper canopy) was excised from each of four to six well-watered individuals and immediately re-cut under water. The newly re-cut end of the branch was placed in water and the entire branch with leaves was covered in black plastic bags to ensure full rehydration. Following rehydration overnight, one mature fully expanded leaf per branch was excised and weighed using a high precision balance. Immediately afterwards, the water potential of the leaf was measured using the pressure chamber. This process was repeated several times until at least five points were obtained beyond the point at which zero turgor was attained. Pressure–volume curves were established by plotting the inverse of leaf water potential ($-1/\Psi$) of each sample vs relative water content. Projected leaf area of each leaf was measured using a leaf area metre and leaf dry weight determined after oven drying at 65 °C for 72 h. Leaf relative water content (RWC) was calculated as the following: RWC = ((WT – WD) – (WF – WD))/(WF – WD) × 100, where WT is turgid fresh weight, WD is leaf dry weight and WF is leaf fresh weight. From the pressure–volume curve, leaf water potential at turgor loss point (Ψ_{tlp}), osmotic potential at full turgor ($\pi 100$) and modulus of elasticity (ε) were calculated according to methods described by Bartlett et al. (2012). Leaf capacitance (C_{leaf}) was calculated from the change in volume per change in water potential above turgor loss point. Leaf-saturated water content (LSWC; g g−1) was calculated as the mass of leaf water (WT – WD) divided by leaf dry mass (WD).

Growth and final harvest

Measurements of stem basal diameter and height were taken on all plants every 4–6 weeks throughout the first three phases of the experiment. Stem volume (cm^3) was calculated from these

measurements assuming that stem taper was consistent with the shape of a cone. Incremental relative growth rates for stem volume (RGR_{vol}, $cm^3\ cm^{-3}\ day^{-1}$) were calculated using the following equation: $(\log(vol_2) - \log(vol_1))/(t_2 - t_1)$, where t is the measurement day. Species growth rates were compared using RGR_{vol} calculated using growth measurements taken from October 2012 to January 2013. At the end of the final dry-down phase, between 11 and 13 individual plants of each species were removed from the shelter for harvesting upon reaching near-complete canopy death. A total of 18 well-watered plants of each species were harvested concurrently, within the same time period as the droughted plants of each species, respectively.

Leaf carbohydrates

For each species, leaves from between 13 and 18 droughted and well-watered plants were sampled for non-structural carbohydrate (NSC) analysis. Leaves from the mid-upper canopy were sampled from each individual at the time they were harvested (see above). After sampling, leaves were microwaved for 5 s to stop metabolism and oven-dried at 70 °C for 72 h before being ground in ball mill (MM400, Retsch, Hann, Germany). For leaf soluble sugars and leaf starch extraction, we followed the protocol described by Tissue and Wright (1995).

Determining plant dry-down time

Species plant dry-down time (or, 'time-to-Ψ_{crit}') was defined as the time it took plants of each species to desiccate from a common level of soil water deficit, measured 4 weeks after the start of the final dry-down phase, to water potentials corresponding to $stemP_{88}$ in the three angiosperms, and $stemP_{50}$ in the conifer. Previous studies suggest these levels of water potential/xylem tension correspond to hydraulic function at or close to plant death (Brodribb and Cochard 2009, Barigah et al. 2013, Urli et al. 2013), although other studies suggest lethal water potentials occur closer to $stemP_{95}$ in some angiosperms (Li et al. 2016). For each species, the average time-to-Ψ_{crit} across individuals was calculated from a quadratic function fitted to the relationship between time (days) and midday leaf water potential measured during the course of the final dry-down phase (see Supplementary Figure S1 available as Supplementary Data at *Tree Physiology* Online).

Statistical analysis

For each species, the relationship between stem hydraulic conductivity and water potential was fitted with a 'Weibull' curve using the 'fitcond' function in the *fitplc* package in R (Duursma and Choat 2017), from which the water potential corresponding to 50% and 88% loss in conductivity, referred to as $stemP_{50}$ and $stemP_{88}$, respectively, was calculated. In each case, bootstrap 95% confidence intervals (CIs) were calculated and species differences were deemed significant if CIs did not overlap.

The response of stomatal conductance (g_s) to increasing water potential was determined for each species using a 3-parameter sigmoidal function fitted to data collected during each of the drought phases, including the final dry-down. The stomatal-hydraulic safety margin was calculated for each species as the difference between the water potential at g_sP_{90} and the water potential at $stemP_{50}$. For each species, differences in biomass and leaf NSCs between drought and well-watered plants at final harvest were tested using one-way analysis of variance in R using log-transformed data.

Results

Growth and gas exchange

Under well-watered conditions, relative rates of stem volume growth (RGR_{vol}, $cm\ cm^{-3}\ day^{-1}$) measured over spring–summer (2012–13) varied (although not significantly, f-value = 1.5, P = 0.27) among the four species (Table 1). The RGR_{vol} of the three angiosperms varied according to their ecological niches, with the riverine species Cacu having the highest RGR_{vol} (5.98×10^{-4} units) and the low-rainfall zone Eusi having the lowest ($4.41 \times$

Table 1. Average values for growth, leaf gas exchange and hydraulics traits measured in plants under well-watered conditions and/or during drought. $^*\Psi_{crit}$ = $stemP_{88}$ for the three angiosperms (Cacu, Eusi and Eute) and $stemP_{50}$ for the conifer Pira. Standard errors are given for growth and leaf gas exchange traits; 95% confidence intervals (CIs) are given for $stemP_{50}$ and $stemP_{88}$.

	Unit	n	Cacu	Eusi	Eute	Pira
Well-watered						
RGR_{vol}	$cm^3\ cm^{-3}\ d^{-1} \times 10^{-4}$	4	5.98 ± 0.6	4.41 ± 0.8	4.83 ± 0.7	3.94 ± 0.7
A_{sat} (mean max)	$\mu mol\ m^{-2}\ s^{-1}$	6	21.2 ± 0.5	19.5 ± 1.3	20.4 ± 1.9	20.4 ± 1.6
g_s (mean max)	$mol\ m^{-2}\ s^{-1}$	6	0.33 ± 0.03	0.43 ± 0.04	0.51 ± 0.1	0.33 ± 0.4
Drought response						
g_sP_{90}	MPa		−2.26	−3.46	−2.64	−1.73
min g_s	$mmol\ m^{-2}\ s^{-1}$	6	13.5 ± 3.1	19.7 ± 9.5	12.6 ± 3.1	1.9 ± 2.6
$StemP_{50}$	MPa		−3.02 (−2.6, −3.5)	−4.28 (−3.5, −4.9)	−4.31 (−3.8, −4.8)	−4.09 (−4.1, −4.1)
$StemP_{88}$	MPa		−5.52 (−4.5, −7.7)	−6.66 (−5.9, −7.7)	−6.64 (−5.6, −9.2)	−4.45 (−4.4, −4.5)
$g_sP_{90} - stemP_{50}$	MPa		0.76	0.82	1.67	2.36
$g_sP_{90} - stem\Psi_{crit}$	MPa		3.13	3.2	4.0	2.36
Dry-down time-to-Ψ_{crit}^*	days		39	57	56	156

10^{-4} units). The plantation conifer Pira had the lowest RGR_{vol} of all four species (3.94×10^{-4} units). In contrast, maximum rates of photosynthesis (A_{sat}) and stomatal conductance (g_s) were strikingly similar across the four species (Table 1).

Drought tolerance traits

The four species differed in a range of traits related to drought tolerance. The water potential at critical levels of hydraulic dysfunction (i.e., $stemP_{50}$ in the conifer Pira and $stemP_{88}$ in the three angiosperms) was highest in Pira (−4.09 MPa) and significantly lower in the three angiosperms (Cacu = −5.52 MPa; Eute = −6.64 MPa; Eusi = −6.66 MPa) (Figure 1 and Table 1). The sensitivity of stomata to increasing drought varied among species, with the water potential at 90% stomatal closure (g_sP_{90}) ranging from −1.73 MPa for the most sensitive species (Pira) to −3.46 MPa for the least sensitive species (Eusi) (Figure 2 and Table 1). The difference between the water potential at stomatal closure (g_sP_{90}) and $stemP_{50}$ was the greatest for Pira (2.36 MPa) and Eute (1.67 MPa) and the smallest for Cacu (0.76 MPa) and Eusi (0.82 MPa). In contrast, the difference between the water potential at stomatal closure (g_sP_{90}) and Ψ_{crit} was the greatest for Eusi (−4.0 MPa) and the smallest for Pira (2.36 MPa) (Table 1).

Pressure–volume traits differed strongly between the three angiosperms and the conifer, but were similar among the angiosperms (Table 2). Leaf-saturated water content (LSWC) and capacitance (C_{leaf}) were much higher in Pira (LSWC = 2.37 g g^{-1}; C_{leaf} = 2.76 mol m^{-2} MPa^{-1}) than the angiosperm species (LSWC ranged from 1.23 g g^{-1} for Eusi to 1.64 g g^{-1} for Cacu; C_{leaf} ranged from 0.41 mol m^{-2} MPa^{-1} for Eute to 0.81 mol m^{-2} MPa^{-1} for Cacu). Similarly, traits such as the water potential at leaf turgor loss (TLP), the solute potential at full turgor (Π_o) and bulk modulus of elasticity (ε) were much lower (less negative for TLP and Π_o) for Pira (TLP = −1.07; Π_o = −0.64; ε = 4.9 MPa) compared with the angiosperms (TLP ranged from −2.04 MPa for Eute to −2.57 MPa for Eusi; Π_o ranged from −1.56 MPa for Eute to −1.86 MPa for Eusi; ε ranged from 18.0 MPa for Eute to 23.8 MPa for Cacu).

Response to repeated drought–recovery cycles

The level of drought stress incurred by plants during the first drought event varied among species. All species showed a decrease in A_{sat} and g_s in response to water deficit (see Supplementary Figures S2 and S3 available as Supplementary Data at *Tree Physiology* Online). At the peak of the first drought event, minimum water potentials were lower in the three angiosperm species (Cacu = −3.1 MPa; Eusi = −3.4 MPa; Eute = −2.6 MPa) compared with the conifer Pira (−1.5 MPa) (Figure 3). Referencing each species vulnerability curve (Figure 1), these water potentials corresponded to a predicted loss in stem hydraulic conductance ranging from 51% for Cacu, 33% for Eusi, 17% for Eute and 0% for Pira. These levels of predicted hydraulic dysfunction were related to the water potential difference between g_sP_{90} and $stemP_{50}$ across species (r^2 = 0.9, P = 0.05; Supplementary Figure S4 available as Supplementary Data at *Tree Physiology* Online). The cumulative impact of the first and second drought events caused a significant reduction in growth (measured in terms of stem volume recorded at the start

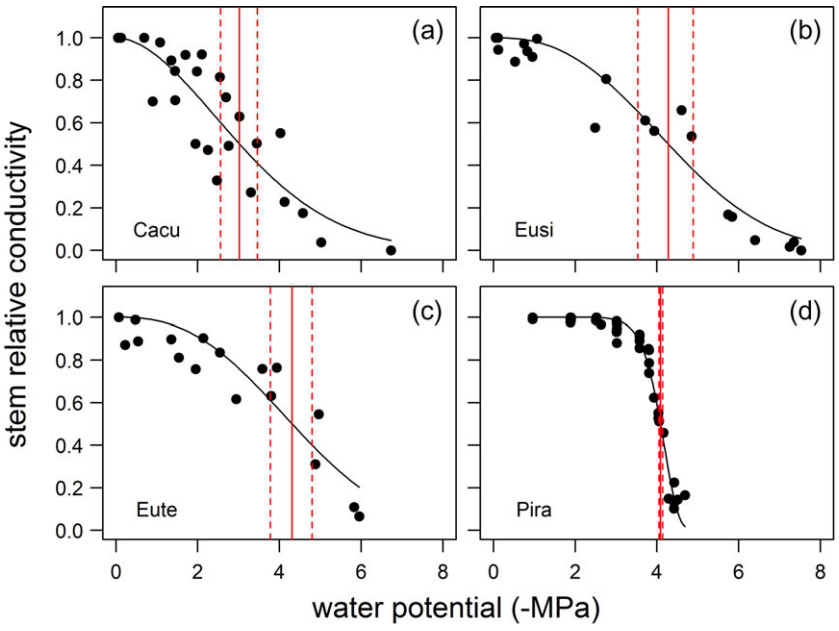

Figure 1. Stem hydraulic vulnerability curves for the species examined in this study. Panels (a), (b), (c) and (d) show stem vulnerability data for Cacu, Eusi, Eute and Pira, respectively. In each panel, the water potential at 50% loss in conductance and associated confidence intervals are indicated by the vertical red line and associated vertical red dashed lines, respectively.

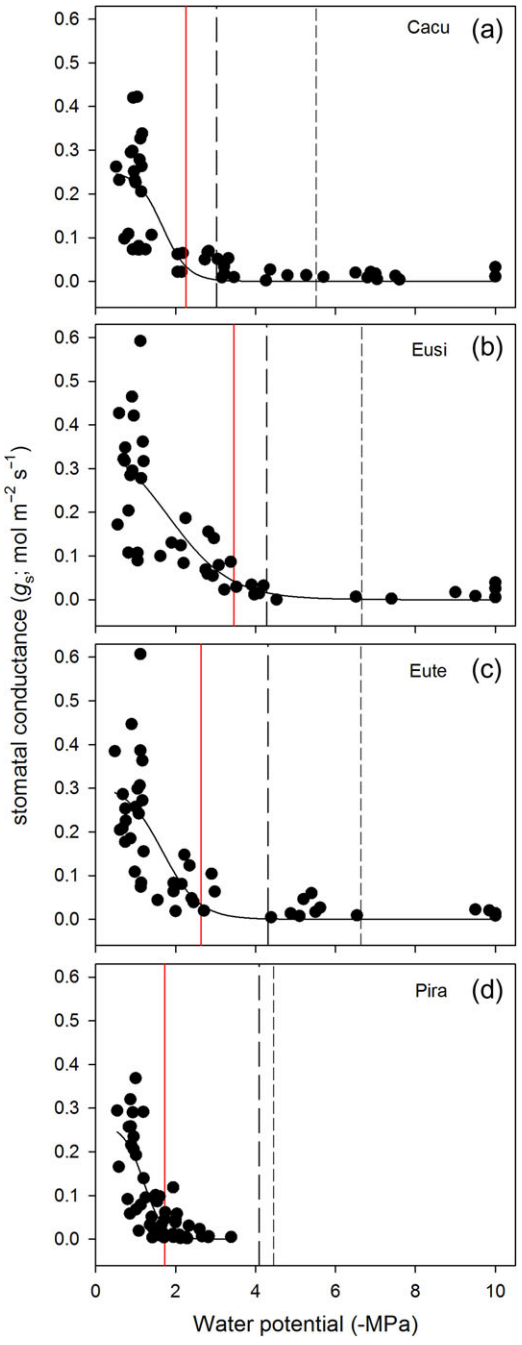

Figure 2. The response of stomatal conductance (g_s) to decreasing water potential during drought recorded for each species; Cacu (a), Eusi (b), Eute (c) and Pira (d). In each panel, the vertical red line indicates the water potential at 90% loss of g_s from mean maximum values, while the long-dashed and short-dashed vertical lines indicate the water potential at stemP_{50} and stemP_{88}, respectively.

of the final drought phase) in droughted plants compared with well-watered controls in only two of the four species (Cacu and Eute, Figure 4). At the end of the repeated drought–recovery cycles, mean plant stem volume (±SE) was 187 ± 16 cm^3, 71.6 ± 5.0 cm^3, 144 ± 9.1 cm^3 and 90.8 ± 3.6 cm^3 for Cacu, Eusi, Eute and Pira, respectively.

Final dry-down phase

For all species, leaf photosynthesis and stomatal conductance decreased as water potentials became more negative during the final dry-down phase (see Supplementary Figures S2 and S3 available as Supplementary Data at *Tree Physiology* Online). The mean length of time that species spent at zero or negative photosynthesis before Ψ_{crit} was relatively short for the three angiosperms (14, 16 and 14 days for Cacu, Eusi and Eute, respectively) and longer for the conifer Pira (82 days). The average (±SE) minimum rate of stomatal conductance (g_s; mmol m^{-2} s^{-1}) was the lowest for Pira (1.9 ± 2.6) and the highest for Eusi (19.7 ± 9.5).

The overall time (days) it took plants to dry-down from a common level of soil water deficit to critical levels of water stress were similar among the three angiosperms (39, 57 and 56 days to stemP_{88} for Cacu, Eusi and Eute, respectively) and longer in the conifer (156 days to stemP_{50}) (Table 1 and Figure 3). Across species, there was a trend of increasing plant dry-down time-to-Ψ_{crit} with increasing stomatal-hydraulic safety (Figure 5). Compared with the three angiosperms, the longer dry-down time-to-Ψ_{crit} recorded for Pira was associated with higher leaf capacitance and lower minimum stomatal conductance (Figure 5). In contrast, the direction of the relationship was less pronounced between plant dry-down time-to-Ψ_{crit} and drought tolerance traits such as g_sP_{90}, stemP_{50} and stemP_{88}, as well as plant biomass traits such as leaf mass fraction and plant size (stem volume) (Figure 5).

For each of the three angiosperms, there was close correspondence between increasing canopy death (percentage brown leaves) and leaf water potential during the final dry-down to mortality phase (Figure 6). In contrast, a poor relationship emerged between the level of leaf browning and water potential for Pira (Figure 6). We were unable to pinpoint the exact water potential associated with mortality. Nevertheless, a subset of plants that were rewatered from levels of drought stress associated with 100% canopy leaf death showed no sign of recovery, with the exception of Eute, in which a few plants showed signs of stem re-sprouting at 2–4 weeks later (see Supplementary Table S1 available as Supplementary Data at *Tree Physiology* Online).

Final biomass and NSCs

Plant biomass ratios were largely unaltered by the three drought events, with the sole exception of Cacu (Table 3). At final harvest, the leaf mass fraction was significantly lower (12.5%) and the root mass fraction was higher (9.7%), but not significantly, in droughted plants of Cacu compared with well-watered controls. At final harvest, a significant reduction in leaf soluble sugars was observed in droughted plants of each species compared with well-watered controls, respectively (Table 4 and Figure 7). In contrast, there were no significant differences in leaf starch between droughted and well-watered plants of any species at the end of the final dry-down phase (Table 4 and Figure 7). Across species, the level of the reduction in leaf soluble sugars and leaf starch

Table 2. Pressure–volume traits (species means ± SE) measured in well-watered plants ($n = 6$) of each species.

	Abbreviation	Unit	Cacu	Eusi	Eute	*Pira*
Saturated water content	LSWC	$g\ g^{-1}$	1.64 ± 0.07	1.23 ± 0.04	1.31 ± 0.03	2.37 ± 0.04
Turgor loss point	TLP	MPa	−2.26 ± 0.11	−2.57 ± 0.11	−2.04 ± 0.11	−1.07 ± 0.14
Solute potential	Π_o	MPa	−1.84 ± 0.11	−1.86 ± 0.1	−1.56 ± 0.1	−0.64 ± 0.11
Elastic modulus	ε	MPa	23.8 ± 1.5	18.7 ± 0.4	18.0 ± 0.7	4.9 ± 0.5
Capacitance	C_{leaf}	$mol\ m^{-2}\ MPa^{-1}$	0.81 ± 0.12	0.58 ± 0.03	0.41 ± 0.01	2.76 ± 0.38

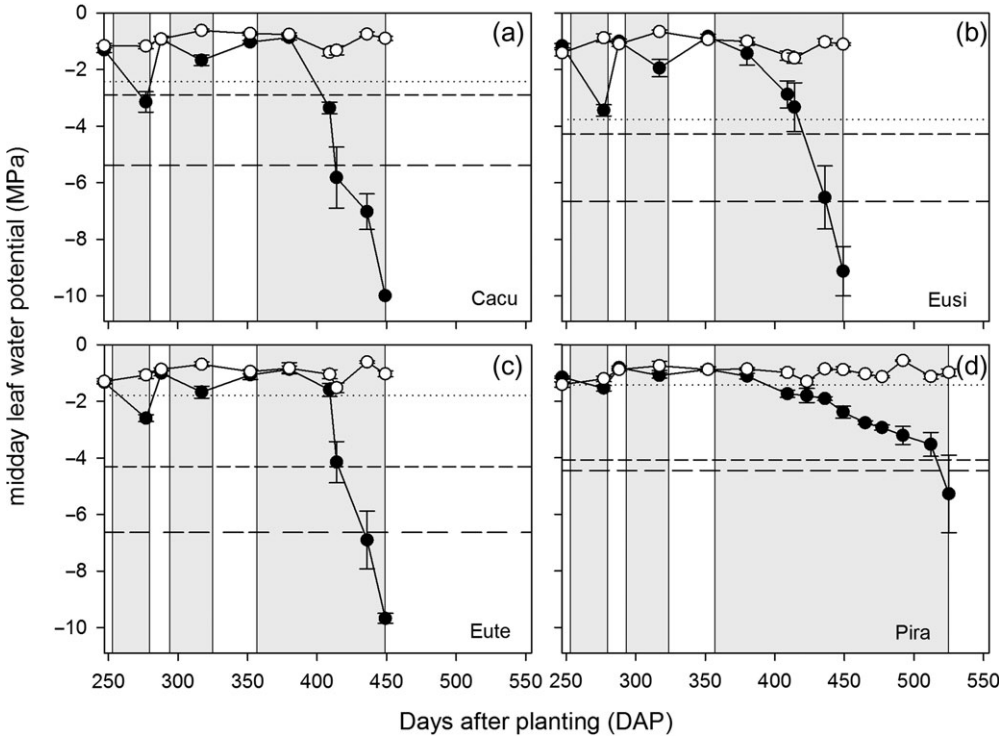

Figure 3. Plots showing changes in midday leaf water potential recorded in droughted (filled circles) and well-watered (empty circles) plants of each species: Cacu (a), Eusi (b), Eute (c) and Pira (d), during the course of the experiment. The light grey shaded areas in each panel represent the first, second and extended drought phases, respectively. In each panel, the dotted horizontal line represents the water potential at stomatal closure, while the short- and long-dashed horizontal lines represent the water potential at $stemP_{50}$ and $stemP_{88}$, respectively. Error bars represent SE.

concentrations was not related to species stomatal-hydraulic safety margin or time-to-Ψ_{crit} (Figure 8).

Discussion

The four species examined in this study showed a range of growth and drought response strategies that in combination with water storage capacitance and drought tolerance traits influenced the duration and intensity of drought stress. Canopy death, as defined by leaf browning, was coincident with water potentials associated with loss of xylem hydraulic conductance due to cavitation in the three angiosperm species. In the conifer species, the occurrence of leaf browning was lagged from extensive cavitation in the stem. At the end of the final dry-down phase, we did not observe a reduction in leaf starch reserves in any species, irrespective of plant dry-down time to critical levels of hydraulic failure.

Species growth and drought response strategies

Species varied in their growth strategies under optimal conditions, with the highest and lowest rates of stem volume growth exhibited by Cacu and Pira, respectively. The level of drought stress incurred during the first and second drought events varied among the four species, despite being dried down to approximately the same level of soil water deficit. All four species showed a reduction in stomatal conductance following bulk turgor loss (Meinzer et al. 2016), although we acknowledge that the mismatch in water potentials at TLP and stomatal closure recorded in three of the four species possibly arose as a result of having estimated TLP in well-water plants and g_sP_{90} in drought-hardened plants. Nevertheless, the narrower hydraulic safety margins exhibited by the three angiosperms is typical of plants that allow water potentials to fall to levels associated with embolism formation during drought (Tardieu and Simonneau

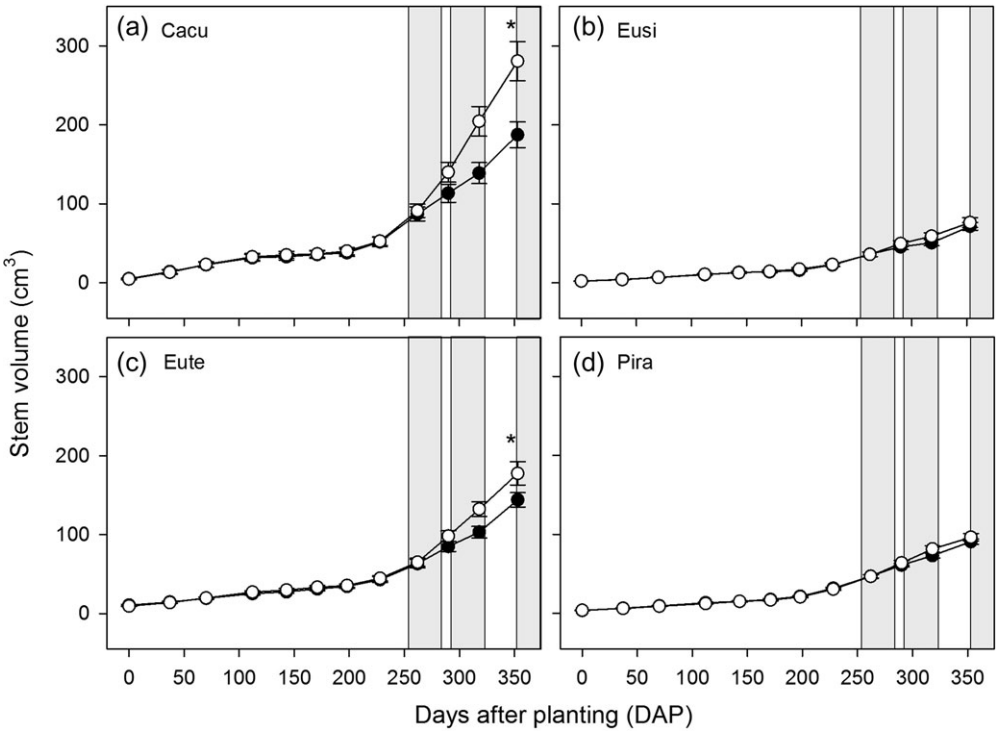

Figure 4. Plots showing changes in mean stem volume (±SE) in drought (filled circles) and well-watered (empty circles) plants of each species: Cacu (a), Eusi (b), Eute (c) and Pira (d), during the experiment up to the start of the final dry-down phase. In each panel, the light grey shaded areas indicate the first, second and (the start of the) final drought phase. Significant differences ($P < 0.05$) in stem volume between drought and well-watered plants at the start of the final dry-down phase are indicated by an asterisk.

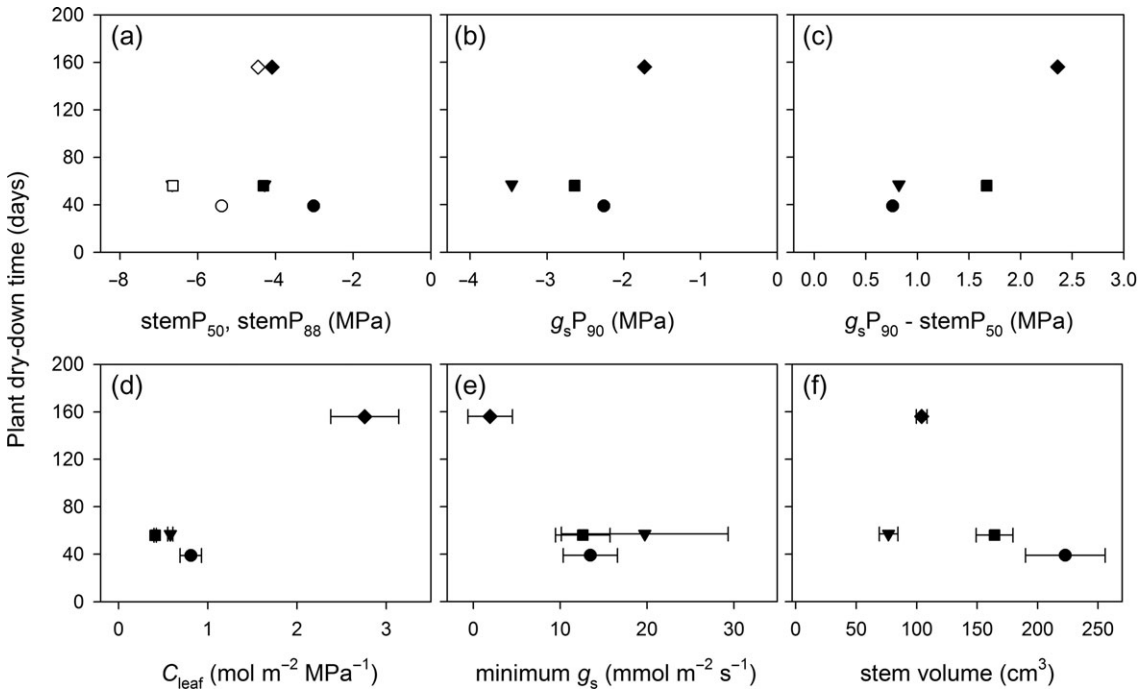

Figure 5. Cross-species relationships between selected hydraulic and biomass traits and plant dry-down time-to-Ψ_{crit} recorded during the final dry-down phase. In each panel, different symbols correspond to the four species examined: circles = Cacu, downward triangles = Eusi, squares = Eute and diamonds = Pira. In plot (a), the solid and open symbols refer to $stemP_{50}$ and $stemP_{88}$, respectively.

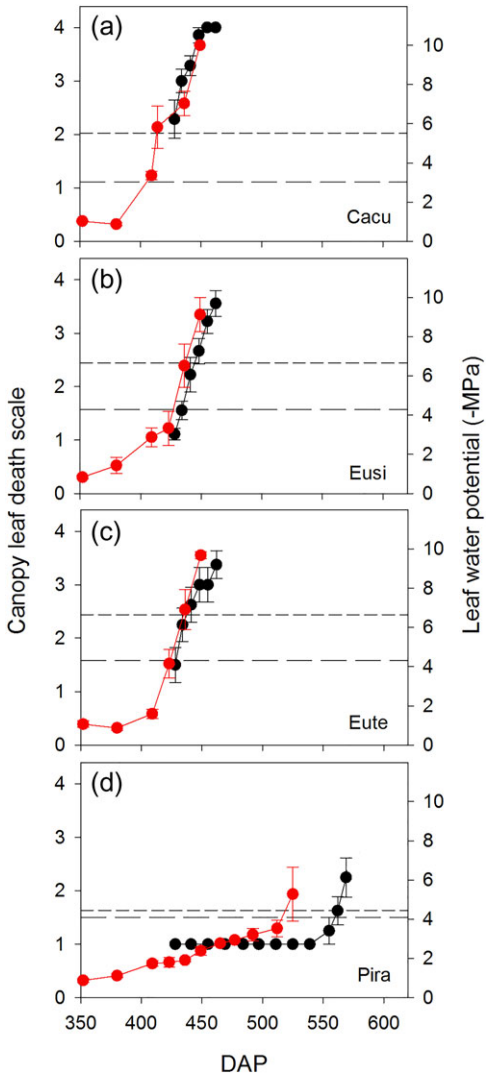

Figure 6. Plots showing close correspondence between a score of canopy leaf browning (black symbols) and leaf water potential (red symbols) during the final dry-down phase for the three angiosperm species: Cacu (a), Eusi (b) and Eute (c), but not for the conifer Pira (d). The scale ranges from 0 (0% of leaves dead) to 4 (100% of leaves dead). In each panel, the short- and long-dashed vertical lines indicate the water potential at stemP_{50} and P_{88}, respectively.

1998, Skelton et al. 2015, Martinez-Vilalta and Garcia-Forner 2017). Consequently, at the peak of the first drought event, the three angiosperms reached water potentials that on average were predicted to cause 17–50% loss of stem hydraulic function. These levels of drought stress had a significant negative effect on sapling growth rates in two of the angiosperms (Cacu and Eute) during subsequent recovery cycles. This reduced rate of growth might be related to more conservative stomatal regulation in response to drought, as has been observed in other temperate tree species in the field (Dietrich et al. 2018). Reduced levels of gas exchange may be a consequence of incomplete hydraulic recovery due to residual xylem embolisms following the first drought event (Blackman et al. 2009, Brodribb and Cochard 2009, Martorell et al. 2014). Alternatively, it might indicate changes in allocation that decouple growth from assimilation, in particular in favour of carbon storage to various carbon sinks (Wurth et al. 2005, Muller et al. 2011, Fatichi et al. 2014, Korner 2015) including to roots (Padilla and Pugnaire 2007), although the observed increase in root mass fraction for drought Cacu plants was not significantly different from controls.

In contrast to the three angiosperm species, the conifer Pira was characterized by highly sensitive stomata that regulated plant water status at high water potentials in response to drought. This conservative stomatal behaviour (Tardieu and Simonneau 1998), coupled with moderate embolism resistance (stemP_{50} similar to the two eucalypts), resulted in Pira having the widest hydraulic safety margin of the four species examined. Similarly wide hydraulic safety margins have been observed in other conifer species (Choat et al. 2012, Martin-StPaul et al. 2017). In effect, stringent stomatal control prevented the loss of hydraulic conductance during the first drought event. Subsequently, rewatered plants without hydraulic impairment would have been able to rapidly restore canopy transpiration, which may help explain the lack of reduced growth observed for Pira during the repeated drought-recovery cycles.

Drought avoidance traits contributed to longer dry-down times

Pira leaves (needles) exhibited a larger LSWC (more water per unit dry weight) and C_{leaf} than the three angiosperm species. A strong ($r^2 = 0.92$) correlation between LSWC and C_{leaf} across the four species suggests these traits are coupled. Similarly, Ogburn and Edwards (2012) found a significant relationship between these variables in a comparison of 25 species while highlighting their contribution to leaf succulence. A larger capacitance means a larger buffering capacity for Pira when water supply becomes limiting, which likely contributed to the longer dry-down time for Pira compared with the three angiosperms. In other studies, larger capacitance has been shown to contribute to longer desiccation time in excised branches of diverse tropical (Borchert and Pockman 2005) and temperate (Gleason et al. 2014) species, and is a key component of models predicting the time it takes plants to reach critical levels of drought stress (Blackman et al. 2016).

Somewhat unexpectedly, plant dry-down time was unrelated to embolism resistance (i.e., stemP_{50} or stemP_{88}) across the four species. This may be due in part to the influence of contrasting hydraulic strategies exhibited by the three angiosperms and the conifer Pira, with the conifer in particular exhibiting traits associated with a drought avoidance strategy (Pivovaroff et al. 2016). In line with these contrasting strategies, there was a strong trend of plant dry-down time increasing with increasing breadth of the stomatal-hydraulic safety margin expressed relative to the water potential at stemP_{50}. When expressed relative to the water potential at stemP_{88}, the stomatal-hydraulic safety

Table 3. Average (±SE) growth and biomass characteristics of well-watered ($n = 18$) and drought plants ($n = 11–13$) of each species harvested at the end of each species final dry-down phase. Bolded values indicate significant differences in biomass allocation between treatments ($P < 0.05$).

		Cacu		Eusi		Eute		Pira	
		WW	D	WW	D	WW	D	WW	D
Height	m	2.51 ± 0.14	1.82 ± 0.09	1.24 ± 0.12	1.18 ± 0.05	1.52 ± 0.09	1.57 ± 0.06	1.17 ± 0.06	1.11 ± 0.02
Basal diameter	cm	3.47 ± 0. 2	2.1 ± 0.1	1.84 ± 0.1	1.6 ± 0.1	2.6 ± 0.1	2.0 ± 0.1	2.3 ± 0.04	1.9 ± 0.03
Volume	cm^3	867 ± 111	223 ± 33	138 ± 46	77 ± 8	315 ± 74	164 ± 15	168 ± 12	104 ± 4
Leaf dry mass	g	314 ± 31	98 ± 11	69 ± 17	56 ± 2.8	63 ± 19	47 ± 12	94 ± 4.5	69 ± 2.4
Branch dry mass	g	145 ± 19	50 ± 8	64 ± 21	45 ± 2	37 ± 11	31 ± 7	23 ± 2	15 ± 1
Stem dry mass	g	307 ± 32	114 ± 14	82 ± 25	58 ± 5.8	149 ± 30	107 ± 8.6	94 ± 6.2	70 ± 2.8
Root dry mass	g	555 ± 61	213 ± 19	208 ± 23	178 ± 20	302 ± 46	201 ± 11	175 ± 10	125 ± 6.0
Total dry mass	kg	1.32 ± 0.13	0.48 ± 0.05	0.42 ± 0.08	0.34 ± 0.03	0.55 ± 0.11	0.39 ± 0.03	0.39 ± 0.02	0.28 ± 0.01
Biomass ratios									
Leaf mass		**0.24** ± 0.01	**0.21** ± 0.01	0.16 ± 0.01	0.17 ± 0.01	0.10 ± 0.01	0.11 ± 0.01	0.25 ± 0.01	0.25 ± 0.01
Branch mass		0.12 ± 0.01	0.10 ± 0.01	0.13 ± 0.01	0.14 ± 0.02	0.06 ± 0.01	0.08 ± 0.01	0.06 ± 0.004	0.05 ± 0.003
Stem mass		0.35 ± 0.01	0.34 ± 0.01	0.31 ± 0.02	0.32 ± 0.02	0.33 ± 0.01	0.36 ± 0.01	0.30 ± 0.01	0.30 ± 0.01
Root mass		0.41 ± 0.02	0.45 ± 0.01	0.54 ± 0.02	0.51 ± 0.03	0.57 ± 0.02	0.53 ± 0.02	0.45 ± 0.02	0.45 ± 0.01

Table 4. Mean leaf carbohydrate concentrations (±SE) measured in well-watered and drought plants at the end of each species dry-down phase.

		Cacu		Eusi		Eute		Pira	
	Unit	WW	D	WW	D	WW	D	WW	D
Starch	$g\ g^{-1}$	58.2 ± 3.3	53.8 ± 3.4	71.3 ± 4.9	58.5 ± 2.1	57.1 ± 5.1	67.7 ± 3.3	63.6 ± 6.2	59.4 ± 2.6
Soluble sugars	$g\ g^{-1}$	67.6 ± 2.9	16.1 ± 3.3	152 ± 5.7	77.5 ± 9.4	98.0 ± 5.2	45.0 ± 6.2	74.0 ± 2.7	33.9 ± 2.3
TNCs	$g\ g^{-1}$	126 ± 5.5	69.9 ± 3.9	223 ± 8.4	136 ± 8.3	155 ± 8.1	113 ± 5.4	138 ± 6.8	93.3 ± 4.0

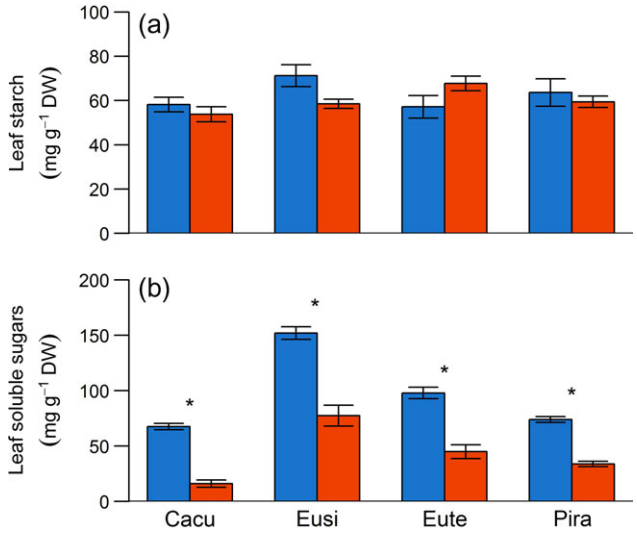

Figure 7. Mean (±SE) concentrations of leaf starch (a) and leaf soluble sugars (b) in well-watered (blue bars) and drought (red bars) plants of each species at the end of the final dry-down phase. Asterisk denote significant differences between treatments ($P < 0.05$).

increased substantially for the three angiosperms but remained roughly the same for the conifer, which in effect changed the species rank order of stomatal-hydraulic safety and decoupled its relationship with dry-down time. Nevertheless, given the strong association across species between stomatal closure and incipient decline in hydraulic function due to embolism (Skelton et al. 2018, Li et al. 2018*b*), we argue that stomatal-hydraulic safety expressed relative to a common level of water stress at stemP_{50}, which represents the steepest portion of the vulnerability curve, is functionally more relevant to understanding species drought response strategy (Skelton et al. 2015, Martin-StPaul et al. 2017, Wason et al. 2018).

Other traits that were likely to contribute to differences in plant desiccation time between species include the minimum leaf conductance (g_{min}, mmol m^{-2} s^{-1}), which is known to be very low in species of *Pinus* and relatively high in genera such as *Eucalyptus* from the family Myrtaceae (Duursma et al. 2018). Consistent with this, minimum rates of stomatal conductance (min g_s; mol m^{-2} s^{-1}) measured toward the end of the final dry-down phase, were significantly lower for Pira than the three angiosperms. Slow rates of desiccation during extended periods of drought may also be dependent on whether plants can hydraulically isolate roots from rapidly drying soil (North and Nobel 1997), which is likely to be true of Pira considering that pre-dawn water potentials in droughted plants were significantly less negative than soil water potentials toward the end of the final dry-down phase (Drake et al. 2017).

Additionally, variation in plant size and total leaf surface area might have contributed to the observed species differences in

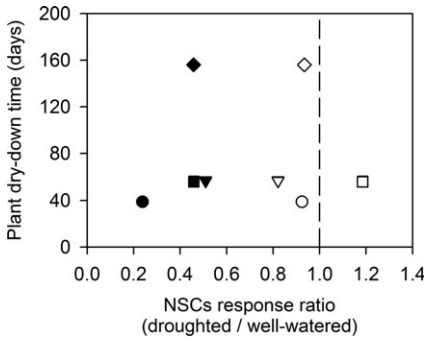

Figure 8. Cross-species relationships between the response ratio of leaf starch (filled symbols) and leaf soluble sugar (open symbols) concentrations in well-watered and droughted plants of Cacu (circles), Eusi (downward triangles), Eute (squares) and Pira (diamonds), measured at the end of the experiment.

plant dry-down time. However, the relationship between plant dry-down time and both the average size (expressed as stem volume) and average leaf mass ratio of saplings was not significant across the four species, although we acknowledge that our biomass measurements may not have adequately captured species variation in total leaf area, most likely as a result of species differences in leaf form. Modelling analysis of plant dry-down times indicate that differences in leaf area will drive differences in the rate of plant water loss before and after stomatal closure (Mackay et al. 2015, Martin-StPaul et al. 2017). Nevertheless, if we assume that the contribution of leaves and stems to whole plant water loss are the same during drought, then the time to critical levels of drought stress will not just depend on total leaf area but also on the amount of water available in the plant (see Blackman et al. 2016). Further detailed experiments are needed to elucidate the dynamics of water loss from different plant organs, not just from stems (Tyree and Yang 1990) or shoots (Borchert and Pockman 2005, Gleason et al. 2014), during all phases of drought.

It is important to acknowledge that plant desiccation time recorded for Pira was likely extended, compared with the three angiosperms, due to plants surviving into the cooler winter months associated with lower evaporative demand. Nevertheless, it remains clear that Pira exhibits a range of traits including early stomatal closure, slow rates of desiccation and leaf succulence that allowed plants to delay the onset of critical hydraulic failure during drought. Although rapid dry-down times were observed in the angiosperm species using potted plants, albeit in large volume (75 l) containers, the risk of exposure to desiccation in large mature trees is likely reduced for Cacu by its occurrence in riparian zones and for the two eucalypt species via their access to underground water reserves and large water storage capacitance. Thus, when estimating plant dry-down times in mature plants in the field, it is important to also consider traits such as rooting depth that determine plant water availability in the soil, and the environmental variables that influence the likelihood of drought stress occurring (Mitchell et al. 2016, Feng et al. 2018). Overall our findings highlight the need to incorporate multiple traits and processes related to drought resistance (e.g., hydraulic vulnerability) and avoidance (e.g., capacitance and/or stomatal closure) when making predictions about the duration of drought before hydraulic failure and defining species overall drought tolerance.

The mechanism of mortality

Strong correspondence between decreasing water potential and canopy browning in the three angiosperms suggests a hydraulic mechanism of progressive leaf death in these species. Interestingly, our measure of complete canopy death occurred at water potentials well beyond $stemP_{88}$ in all three angiosperms, although we acknowledge the difficulty in determining plant death from visual estimates of leaf browning without quantifying thresholds of irrecoverable drought stress (Brodribb and Cochard 2009). A similar response has been observed in temperate woody angiosperms (Blackman et al. 2009) and suggests that some plants are able to maintain a small proportion of 'green' leaf area under severe drought stress, despite severe leaf and stem hydraulic dysfunction. It also suggests that theoretical plant morality thresholds in angiosperms, namely $stemP_{88}$ (Resco et al. 2009, Urli et al. 2013), may be conservative (Li et al. 2016). Although we were unable to clearly define the exact lethal water potential in our study species, plants were assumed to be dead (non-recoverable) at 100% canopy death. Nevertheless, a few drought plants of one species (Eute) showed signs of stem re-sprouting 2–4 weeks after soil re-wetting, again indicating that plants may show some capacity to maintain living tissue (at least in the short term) despite near-complete loss in xylem conductance. This level of resilience is not entirely surprising in *Eucalyptus*, given the genus is well known for containing species with a high capacity for re-sprouting following fire and drought (Zeppel et al. 2015).

The contrasting drought response strategies of the four species in this study did not differentially affect concentrations of leaf starch and soluble sugars in drought and well-watered plants at the end of the experiment. In other words, and contrary to our expectations, we found no link between the duration of drought and the level of carbohydrate depletion observed at the end of the final dry-down phase. Also, we did not observe a significant decrease in leaf starch in droughted plants of any species, which is in contrast to previous drought studies (Adams et al. 2013, Duan et al. 2013, Mitchell et al. 2013) and a meta-analysis of seasonal variation in NSCs (Martinez-Vilalta et al. 2016), although the authors also report strong variability in the level of seasonal starch depletion across plant functional types. In the current study, the lack of a reduction in leaf starch observed in plants of all species may have been due to processes linked to hydraulic limitation of phloem transport (Sevanto 2018). Alternatively, it may have been due to an insufficiently long period of zero or negative carbon balance recorded in our plants during the final dry-down phase.

It is likely that all plants in our experiment died as a result of catastrophic hydraulic failure and severe tissue desiccation. This finding supports numerous studies that have observed a hydraulic-related mechanism of drought-induced dieback and/or mortality in manipulative and field studies (Brodribb and Cochard 2009, Nardini et al. 2013, Anderegg et al. 2015, Johnson et al. 2018, Li et al. 2018*a*). However, we note that carbon depletion may play a role in mortality during longer periods of drought (Galiano et al. 2012, Dai et al. 2018), that the interplay between carbon and hydraulic processes during drought can be complex (Nardini et al. 2016, Adams et al. 2017) and furthermore that in some instances trees in the field show low levels of both hydraulic dysfunction and carbon depletion during severe drought (Dietrich et al. 2018). We suggest that future work in this area considers how diverse species with a range of traits linked to stomatal sensitivity and drought tolerance thresholds respond to acute (short) vs chronic (long) drought stress in the glasshouse and in the field when attempting to identify ecologically relevant mechanisms of drought mortality.

Supplementary Data

Supplementary data for this article are available at *Tree Physiology* Online.

Acknowledgments

This experiment was supported by the Hawkesbury Institute for the Environment and Western Sydney University and the ANR-10-EQPX-16, XYLOFOREST. We thank Burhan Amiji and Craig Barton for their excellent technical support and help maintaining the site. Randol Villalobos-Vega, Nicolas Boulain, Melanie Zeppel, Markus Nolf, Alicia Cook and Honglang Duan contributed to the photosynthesis, leaf water potential and/or leaf pressure–volume measurements.

Conflict of interest

None declared.

References

Adams HD, Germino MJ, Breshears DD, Barron-Gafford GA, Guardiola-Claramonte M, Zou CB, Huxman TE (2013) Nonstructural leaf carbohydrate dynamics of *Pinus edulis* during drought-induced tree mortality reveal role for carbon metabolism in mortality mechanism. New Phytol 197:1142–1151.

Adams HD, Zeppel MJB, Anderegg WRL et al. (2017) A multi-species synthesis of physiological mechanisms in drought-induced tree mortality. Nat Ecol Evol 1:1285–1291.

Allen CD, Macalady AK, Chenchouni H et al. (2010) A global overview of drought and heat-induced tree mortality reveals emerging climate change risks for forests. For Ecol Manage 259:660–684.

Allen CD, Breshears DD, McDowell NG (2015) On underestimation of global vulnerability to tree mortality and forest die-off from hotter drought in the Anthropocene. Ecosphere 6:1–55.

Anderegg WRL, Berry JA, Smith DD, Sperry JS, Anderegg LDL, Field CB (2012) The roles of hydraulic and carbon stress in a widespread climate-induced forest die-off. Proc Natl Acad Sci USA 109:233–237.

Anderegg WRL, Flint A, Huang C-y, Flint L, Berry JA, Davis FW, Sperry JS, Field CB (2015) Tree mortality predicted from drought-induced vascular damage. Nat Geosci 8:367–371.

Barigah TS, Charrier O, Douris M, Bonhomme M, Herbette S, Ameglio T, Fichot R, Brignolas F, Cochard H (2013) Water stress-induced xylem hydraulic failure is a causal factor of tree mortality in beech and poplar. Ann Bot (Lond) 112:1431–1437.

Barnard DM, Meinzer FC, Lachenbruch B, McCulloh KA, Johnson DM, Woodruff DR (2011) Climate-related trends in sapwood biophysical properties in two conifers: avoidance of hydraulic dysfunction through coordinated adjustments in xylem efficiency, safety and capacitance. Plant Cell Environ 34:643–654.

Bartlett MK, Scoffoni C, Sack L (2012) The determinants of leaf turgor loss point and prediction of drought tolerance of species and biomes: a global meta-analysis. Ecol Lett 15:393–405.

Bartlett MK, Klein T, Jansen S, Choat B, Sack L (2016) The correlations and sequence of plant stomatal, hydraulic, and wilting responses to drought. Proc Natl Acad Sci USA 113:13098–13103.

Blackman CJ, Brodribb TJ, Jordan GJ (2009) Leaf hydraulics and drought stress: response, recovery and survivorship in four woody temperate plant species. Plant Cell Environ 32:1584–1595.

Blackman CJ, Pfautsch S, Choat B, Delzon S, Gleason SM, Duursma RA (2016) Toward an index of desiccation time to tree mortality under drought. Plant Cell Environ 39:2342–2345.

Borchert R, Pockman WT (2005) Water storage capacitance and xylem tension in isolated branches of temperate and tropical trees. Tree Physiol 25:457–466.

Bourne AE, Creek D, Peters JMR, Ellsworth DS, Choat B (2017) Species climate range influences hydraulic and stomatal traits in Eucalyptus species. Ann Bot (Lond) 120:123–133.

Breda N, Huc R, Granier A, Dreyer E (2006) Temperate forest trees and stands under severe drought: a review of ecophysiological responses, adaptation processes and long-term consequences. Ann For Sci 63: 625–644.

Breshears DD, Cobb NS, Rich PM et al. (2005) Regional vegetation die-off in response to global-change-type drought. Proc Natl Acad Sci USA 102:15144–15148.

Brodribb TJ, Cochard H (2009) Hydraulic failure defines the recovery and point of death in water-stressed conifers. Plant Physiol 149: 575–584.

Brodribb TJ, McAdam SAM (2013) Abscisic acid mediates a divergence in the drought response of two conifers. Plant Physiol 162:1370–1377.

Choat B (2013) Predicting thresholds of drought-induced mortality in woody plant species. Tree Physiol 33:669–671.

Choat B, Drayton WM, Brodersen C, Matthews MA, Shackel KA, Wada H, McElrone AJ (2010) Measurement of vulnerability to water stress-induced cavitation in grapevine: a comparison of four techniques applied to a long-vesseled species. Plant Cell Environ 33:1502–1512.

Choat B, Jansen S, Brodribb TJ et al. (2012) Global convergence in the vulnerability of forests to drought. Nature 491:752–755.

Choat B, Badel E, Burlett R, Delzon S, Cochard H, Jansen S (2016) Noninvasive measurement of vulnerability to drought-induced embolism by X-ray microtomography. Plant Physiol 170:273–282.

Choat B, Brodribb TJ, Brodersen CR, Duursma RA, Lopez R, Medlyn BE (2018) Triggers of tree mortality under drought. Nature 558:531–539.

Clark JS, Iverson L, Woodall CW et al. (2016) The impacts of increasing drought on forest dynamics, structure, and biodiversity in the United States. Glob Chang Biol 22:2329–2352.

Cochard H, Damour G, Bodet C, Tharwat I, Poirier M, Ameglio T (2005) Evaluation of a new centrifuge technique for rapid generation of xylem vulnerability curves. Physiol Plant 124:410–418.

Cochard H, Herbette S, Barigah T, Badel E, Ennajeh M, Vilagrosa A (2010) Does sample length influence the shape of xylem embolism vulnerability curves? A test with the Cavitron spinning technique. Plant Cell Environ 33:1543–1552.

Cochard H, Badel E, Herbette S, Delzon S, Choat B, Jansen S (2013) Methods for measuring plant vulnerability to cavitation: a critical review. J Exp Bot 64:4779–4791.

Dai YX, Wang L, Wan XC (2018) Relative contributions of hydraulic dysfunction and carbohydrate depletion during tree mortality caused by drought. Aob Plants 10. doi: 10.1093/aobpla/plx069.

Dietrich L, Delzon S, Hoch G, Kahmen A (2018) No role for xylem embolism or carbohydrate shortage in temperate trees during the severe 2015 drought. J Ecol 107:334–349.

Dijkstra FA, Carrillo Y, Aspinwall MJ, Maier C, Canarini A, Tahaei H, Choat B, Tissue DT (2016) Water, nitrogen and phosphorus use efficiencies of four tree species in response to variable water and nutrient supply. Plant Soil 406:187–199.

Drake JE, Aspinwall MJ, Pfautsch S et al. (2015) The capacity to cope with climate warming declines from temperate to tropical latitudes in two widely distributed Eucalyptus species. Glob Chang Biol 21:459–472.

Drake JE, Power SA, Duursma RA et al. (2017) Stomatal and non-stomatal limitations of photosynthesis for four tree species under drought: a comparison of model formulations. Agric For Meteorol 247: 454–466.

Duan H, Amthor JS, Duursma RA, O'Grady AP, Choat B, Tissue DT (2013) Carbon dynamics of eucalypt seedlings exposed to progressive drought in elevated CO_2 and elevated temperature. Tree Physiol 33:779–792.

Duan H, Duursma RA, Huang G, Smith RA, Choat B, O'Grady AP, Tissue DT (2014) Elevated CO2 does not ameliorate the negative effects of elevated temperature on drought-induced mortality in Eucalyptus radiata seedlings. Plant Cell Environ 37: 1598–1613.

Duan H, O'Grady AP, Duursma RA, Choat B, Huang G, Smith RA, Jiang Y, Tissue DT (2015) Drought responses of two gymnosperm species with contrasting stomatal regulation strategies under elevated CO_2 and temperature. Tree Physiol 35:756–770.

Duan HL, Chaszar B, Lewis JD, Smiths RA, Huxman TE, Tissue DT (2018) CO_2 and temperature effects on morphological and physiological traits affecting risk of drought-induced mortality. Tree Physiol 38:1138–1151.

Duke NC, Kovacs JM, Griffiths AD, Preece L, Hill DJE, van Oosterzee P, Mackenzie J, Morning HS, Burrows D (2017) Large-scale dieback of mangroves in Australia's Gulf of Carpentaria: a severe ecosystem response, coincidental with an unusually extreme weather event. Mar Freshw Res 68:1816–1829.

Duursma RA, Choat B (2017) fitplc: an R package to fit hydraulic vulnerability curves. J Plant Hydraul 4. https://doi.org/10.20870/jph.2017.e002.

Duursma RA, Blackman CJ, Lopéz R, Martin-StPaul NK, Cochard H, Medlyn BE (2018) On the minimum leaf conductance: its role in models of plant water use, and ecological and environmental controls. New Phytol. 221:693–705.

Engelbrecht BMJ, Comita LS, Condit R, Kursar TA, Tyree MT, Turner BL, Hubbell SP (2007) Drought sensitivity shapes species distribution patterns in tropical forests. Nature 447:80.

Engelbrecht BMJ (2012) Plant ecology: forests on the brink. Nature 491: 675–677.

Fatichi S, Leuzinger S, Korner C (2014) Moving beyond photosynthesis: from carbon source to sink-driven vegetation modeling. New Phytol 201:1086–1095.

Feng X, Ackerly DD, Dawson TE, Manzoni S, Skelton RP, Vico G, Thompson SE (2018) The ecohydrological context of drought and classification of plant responses. Ecol Lett 21:1723–1736.

Fensham RJ, Fairfax RJ (2007) Drought-related tree death of savanna eucalypts: Species susceptibility, soil conditions and root architecture. J Veg Sci 18:71–80.

Fensham RJ, Holman JE (1999) Temporal and spatial patterns in drought-related tree dieback in Australian savanna. J Appl Ecol 36: 1035–1050.

Fu X, Meinzer FC (2018) Metrics and proxies for stringency of regulation of plant water status (iso/anisohydry): a global data set reveals coordination and trade-offs among water transport traits. Tree Physiol 39:122–134.

Galiano L, Martinez-Vilalta J, Sabate S, Lloret F (2012) Determinants of drought effects on crown condition and their relationship with depletion of carbon reserves in a Mediterranean holm oak forest. Tree Physiol 32:478–489.

Gleason SM, Blackman CJ, Cook AM, Laws CA, Westoby M (2014) Whole-plant capacitance, embolism resistance and slow transpiration rates all contribute to longer desiccation times in woody angiosperms from arid and wet habitats. Tree Physiol 34:275–284.

Gleason SM, Westoby M, Jansen S et al. (2016) Weak tradeoff between xylem safety and xylem-specific hydraulic efficiency across the world's woody plant species. New Phytol 209:123–136.

Hacke UG, Sperry JS, Pockman WT, Davis SD, McCulloh KA (2001) Trends in wood density and structure are linked to prevention of xylem implosion by negative pressure. Oecologia 126:457–461.

Jacobsen AL, Ewers FW, Pratt RB, Paddock Iii WA, Davis SD (2005) Do xylem fibers affect vessel cavitation resistance? Plant Physiol 139: 546–556.

Johnson DM, Domec JC, Berry ZC et al. (2018) Co-occurring woody species have diverse hydraulic strategies and mortality rates during an extreme drought. Plant Cell Environ 41:576–588.

Korner C (2015) Paradigm shift in plant growth control. Curr Opin Plant Biol 25:107–114.

Li S, Feifel M, Karimi Z, Schuldt B, Choat B, Jansen S (2016) Leaf gas exchange performance and the lethal water potential of five European species during drought. Tree Physiol 36:179–192.

Li X, Blackman CJ, Rymer PD, Quintans D, Duursma RA, Choat B, Medlyn BE, Tissue DT (2018*a*) Xylem embolism measured retrospectively is linked to canopy dieback in natural populations of *Eucalyptus piperita* following drought. Tree Physiol 38:1193–1199.

Li XM, Blackman CJ, Choat B, Duursma RA, Rymer PD, Medlyn BE, Tissue DT (2018*b*) Tree hydraulic traits are coordinated and strongly linked to climate-of-origin across a rainfall gradient. Plant Cell Environ 41:646–660.

Mackay DS, Roberts DE, Ewers BE, Sperry JS, McDowell NG, Pockman WT (2015) Interdependence of chronic hydraulic dysfunction and canopy processes can improve integrated models of tree response to drought. Water Resour Res 51:6156–6176.

Markesteijn L, Poorter L, Bongers F, Paz H, Sack L (2011) Hydraulics and life history of tropical dry forest tree species: coordination of species' drought and shade tolerance. New Phytol 191:480–495.

Martin-StPaul N, Delzon S, Cochard H (2017) Plant resistance to drought depends on timely stomatal closure. Ecol Lett 20:1437–1447.

Martinez-Vilalta J, Garcia-Forner N (2017) Water potential regulation, stomatal behaviour and hydraulic transport under drought: deconstructing the iso/anisohydric concept. Plant Cell Environ 40:962–976.

Martinez-Vilalta J, Sala A, Asensio D, Galiano L, Hoch G, Palacio S, Piper FI, Lloret F (2016) Dynamics of non-structural carbohydrates in terrestrial plants: a global synthesis. Ecol Monogr 86:495–516.

Martorell S, Diaz-Espejo A, Medrano H, Ball MC, Choat B (2014) Rapid hydraulic recovery in *Eucalyptus pauciflora* after drought: linkages between stem hydraulics and leaf gas exchange. Plant Cell Environ 37:617–626.

McDowell N, Pockman WT, Allen CD et al. (2008) Mechanisms of plant survival and mortality during drought: why do some plants survive while others succumb to drought? New Phytol 178:719–739.

Meinzer FC, Woodruff DR, Marias DE, Smith DD, McCulloh KA, Howard AR, Magedman AL (2016) Mapping 'hydroscapes' along the iso- to anisohydric continuum of stomatal regulation of plant water status. Ecol Lett 19:1343–1352.

Mitchell P, O'Grady AP, Pinkard EA et al. (2016) An eco-climatic framework for evaluating the resilience of vegetation to water deficit. Glob Chang Biol 22:1677–1689.

Mitchell PJ, O'Grady AP, Tissue DT, White DA, Ottenschlaeger ML, Pinkard EA (2013) Drought response strategies define the relative contributions of hydraulic dysfunction and carbohydrate depletion during tree mortality. New Phytol 197:862–872.

Muller B, Pantin F, Genard M, Turc O, Freixes S, Piques M, Gibon Y (2011) Water deficits uncouple growth from photosynthesis, increase C content, and modify the relationships between C and growth in sink organs. J Exp Bot 62:1715–1729.

Nardini A, Battistuzzo M, Savi T (2013) Shoot desiccation and hydraulic failure in temperate woody angiosperms during an extreme summer drought. New Phytol 200:322–329.

Nardini A, Casolo V, Dal Borgo A, Savi T, Stenni B, Bertoncin P, Zini L, McDowell NG (2016) Rooting depth, water relations and non-structural carbohydrate dynamics in three woody angiosperms differentially affected by an extreme summer drought. Plant Cell Environ 39: 618–627.

North GB, Nobel PS (1997) Root-soil contact for the desert succulent Agave deserti in wet and drying soil. New Phytol 135:21–29.

Ogburn RM, Edwards EJ (2012) Quantifying succulence: a rapid, physiologically meaningful metric of plant water storage. Plant Cell Environ 35:1533–1542.

Padilla FM, Pugnaire FI (2007) Rooting depth and soil moisture control Mediterranean woody seedling survival during drought. Funct Ecol 21: 489–495.

Phillips OL, van der Heijden G, Lewis SL et al. (2010) Drought–mortality relationships for tropical forests. New Phytol 187:631–646.

Pivovaroff AL, Pasquini SC, De Guzman ME, Alstad KP, Stemke JS, Santiago LS (2016) Multiple strategies for drought survival among woody plant species. Funct Ecol 30:517–526.

Poot P, Veneklaas EJ (2013) Species distribution and crown decline are associated with contrasting water relations in four common sympatric eucalypt species in southwestern Australia. Plant Soil 364:409–423.

Reich PB (2014) The world-wide 'fast-slow' plant economics spectrum: a traits manifesto. J Ecol 102:275–301.

Reichstein M, Bahn M, Ciais P et al. (2013) Climate extremes and the carbon cycle. Nature 500:287–295.

Resco V, Ewers BE, Sun W, Huxman TE, Weltzin JF, Williams DG (2009) Drought-induced hydraulic limitations constrain leaf gas exchange recovery after precipitation pulses in the C-3 woody legume, *Prosopis velutina*. New Phytol 181:672–682.

Sala A, Woodruff DR, Meinzer FC (2012) Carbon dynamics in trees: feast or famine? Tree Physiol 32:764–775.

Scholz FG, Phillips N, Bucci SJ, Meinzer FC, Goldstein G (2011) Hydraulic capacitance: biophysics and functional significance of internal water sources in relation to tree size. In: Meinzer FC, Lachenbruch B, Dawson TE (eds) Size- and age-related changes in tree structure and function. Springer, Dordrecht, pp 341–361.

Sevanto S (2018) Drought impacts on phloem transport. Curr Opin Plant Biol 43:76–81.

Skelton RP, West AG, Dawson TE (2015) Predicting plant vulnerability to drought in biodiverse regions using functional traits. Proc Natl Acad Sci USA 112:5744–5749.

Skelton RP, Dawson TE, Thompson SE, Shen Y, Weitz AP, Ackerly D (2018) Low vulnerability to xylem embolism in leaves and stems of North American oaks. Plant Physiol 177:1066–1077.

Sperry JS, Donnelly JR, Tyree MT (1988) A method for measuring hydraulic conductivity and embolism in xylem. Plant Cell Environ 11: 35–40.

Tardieu F, Simonneau T (1998) Variability among species of stomatal control under fluctuating soil water status and evaporative demand: modelling isohydric and anisohydric behaviours. J Exp Bot 49:419–432.

Tissue DT, Wright SJ (1995) Effect of seasonal water availability on phenology and the annual shoot carbohydrate cycle of tropical forest shrubs. Funct Ecol 9:518–527.

Torres-Ruiz JM, Cochard H, Mayr S, Beikircher B, Diaz-Espejo A, Rodriguez-Dominguez CM, Badel E, Fernandez JE (2014) Vulnerability to cavitation in *Olea europaea* current-year shoots: further evidence of an open-vessel artifact associated with centrifuge and air-injection techniques. Physiol Plant 152:465–474.

Torres-Ruiz JM, Jansen S, Choat B et al. (2015) Direct X-ray microtomography observation confirms the induction of embolism upon xylem cutting under tension. Plant Physiol 167:40–43.

Tyree MT, Yang SD (1990) Water-storage capacity of *Thuja*, *Tsuga* and *Acer* stems measured by dehydration isotherms. Planta 182: 420–426.

Urli M, Porte AJ, Cochard H, Guengant Y, Burlett R, Delzon S (2013) Xylem embolism threshold for catastrophic hydraulic failure in angiosperm trees. Tree Physiol 33:672–683.

Wason JW, Anstreicher KS, Stephansky N, Huggett BA, Brodersen CR (2018) Hydraulic safety margins and air-seeding thresholds in roots, trunks, branches and petioles of four northern hardwood trees. New Phytol 219:77–88.

Wheeler JK, Huggett BA, Tofte AN, Rockwell FE, Holbrook NM (2013) Cutting xylem under tension or supersaturated with gas can generate PLC and the appearance of rapid recovery from embolism. Plant Cell Environ 36:1938–1949.

Wurth MKR, Pelaez-Riedl S, Wright SJ, Korner C (2005) Non-structural carbohydrate pools in a tropical forest. Oecologia 143:11–24.

Zeppel MJB, Harrison SP, Adams HD et al. (2015) Drought and resprouting plants. New Phytol 206:583–589.